

Physical Limits of Different Models of Cosmic Gamma-Ray Bursts

Gennady S. Bisnovatyi-Kogan^{1,2} *

¹ Space Research Inst. Rus. Acad. Sci, Profsoyuznaya 84/32, Moscow 117997, Russia

² Joint Institute of Nuclear Researches, Dubna, Russia

Abstract The present common view about GRB origin is related to cosmology, what is based on statistical analysis, and on measurements of the redshifts in the GRB optical afterglows of long GRB. No correlation is found between redshifts, GRB spectrum, and total GRB fluence. Comparison of KONUS and BATSE data about statistics and hard X-ray lines is done, and some differences are noted. Hard gamma-ray afterglows, prompt optical spectra, hard X-ray lines measurements could be important for farther insight into GRB origin. Possible possible connection of short GRB with soft gamma repeaters is discussed.

Key words: gamma-rays, X-rays, transients

1 INTRODUCTION

It is generally accepted now that cosmic gamma-ray bursts (GRB) have a cosmological origin. The first cosmological model, based on explosions in active galactic nuclei (AGN) was suggested by Prilutsky & Usov (1975). A mechanism of the GRB origin in the vicinity of a collapsing object based on neutrino-antineutrino annihilation was analyzed by Berezhinsky & Prilutsky (1987). GRB production in supernova explosion was suggested by Bisnovatyi-Kogan et al. (1975). Here we discuss different observational features of GRB, analyze difficulties and problems of their interpretation in the cosmological model, and physical restrictions to their model. At the end we are analyze a possible connection between short GRB and soft gamma repeater (SGR).

2 GRB PHYSICAL MODELS

The GRB models may be classified by two levels. The upper one is related directly to the observational appearance, and include 3 main models.

1. Fireball. **2.** Cannon ball (or gun bullet). **3.** Precessing jets.

The main restrictions are connected with the next (basic) level of GRB model, which is related to energy source, producing a huge energy output necessary for a cosmological GRB model. These class contains 5 main models.

* E-mail: gkogan@mx.iki.rssi.ru

1. (NS+NS), (NS+BH) mergers. This mechanism was investigated numerically by Ruffert and Janka (1998, 1999). Gamma radiation is produced here by $(\nu, \bar{\nu})$ annihilation, and the energy output is not enough to explain most powerful GRB even with account of strong beaming. The energy emitted in the isotropic optical afterglow of GRB 990123 (Akerlof et al. 1999; Kulkarni et al. 1999) is about an order of magnitude larger than the total radiation energy output in this model.

2. Magnetorotational explosion. Magnetorotational explosion, proposed by Paczynski (1998) for a cosmological GRB, had been suggested earlier for the supernova explosion by Bisnovaty-Kogan (1971). Numerical calculations gave the efficiency of a transformation of the rotational energy into the kinetic one at the level of few percent (Ardelyan et al. 1997, 2000). This is enough for the supernovae energy output, but is too low for cosmological GRB.

3. Hypernova. This model denoting very powerful supernova, was suggested in general by Paczynski (1998), and is popular now because traces of the supernova explosions are believed to be found in the optical afterglows of several GRB (Sokolov 2001; Dado et al. 2002; Stanek et al. 2003). The action of strongly magnetized rapidly rotating new born neutron star for production of GRB was considered by Usov (1992). Another hypernova model is based on a collapse of a massive core, formation of a black hole $M_{\text{bh}} \sim 20M_{\odot}$, surrounded by a massive disk with a rapid accretion and appearance of GRB (MacFadyen & Woosley 1999). This modes seems to be most promising now.

4. Magnetized disks around rotating (Kerr) black holes (RBH). This model is based on extraction of rotating energy of RBH when magnetic field is connecting the RBH with the surrounding accretion disk or accretion torus (van Putten 2001).

5. In the model proposed Ruffini et al. (2000) GRB is created by the pair-electromagnetic pulse from an electrically charged black hole surrounded by a baryonic remnant. The main problem here is how to form such a strongly charged BH.

3 BASIC OBSERVATIONAL DATA

3.1 Statistics

Statistical arguments in favor of the cosmological origin of GRB are based on a visual isotropy of GRB distribution on the sky in combination with a strong deviation of $\log N - \log S$ distribution obtained in BATSE observations (Meegan et al. 1992) from the euclidian uniform distribution with the slope 3/2. Similar properties have been obtained in KONUS experiment (Mazets et al. 1980) where the authors explained deviations from 3/2 slope by selection effects. The analysis of KONUS data with account of selection effects made by Higdon and Schmidt (1990) gave the average value $\langle V/V_{\text{max}} \rangle = 0.45 \pm 0.03$; the value 0.5 corresponds to pure uniform distribution. KONUS data had been obtained in conditions of constant background. Similar analysis made by Schmidt (1999) of BATSE data, obtained in conditions of substantially variable background, gave resulting $\langle V/V_{\text{max}} \rangle = 0.334 \pm 0.008$. These two results seems to be in contradiction, because KONUS sensitivity was only 3 times less than that of BATSE, where deviations from the uniform distribution in BATSE data are sill large (Fishman & Meegan 1995).

Detailed statistical analysis and calculation of of BATSE data, divided in 4 classes according to their hardness and calculation of $\langle V/V_{\text{max}} \rangle$ for different classes have been done by Schmidt (2001). In the cosmological model we may expect smaller value of $\langle V/V_{\text{max}} \rangle$ for softer GRB in the case of a uniform sample, because larger red shifts would correspond to softer spectra. The result is quite opposite, and soft GRB have larger $\langle V/V_{\text{max}} \rangle$ than the hard ones, 0.47 and 0.27 respectively. It is supposed by Schmidt (2001) that strong excess of luminosity in hard

GRB overcomes the tendency of the uniform sample. The possibility of decisive role of selection effects (incompleteness of data, statistical errors in estimation of luminosity in presence of the threshold) was analyzed by Harrison et al. (1995), Bisnovatyi-Kogan (1997). The influence of statistical errors in presence of the threshold was analyzed by Bisnovatyi-Kogan (1997). The $\log N - \log S$ curve in presence of statistical errors on the level of average 10 thresholds has a similarity with the BATSE distribution (see Fig. 1 and Fig. 2).

3.2 Optical Afterglows and Red Shifted Lines

The spectra of optical afterglows have shown large red shifts z , up to 4.5, indicating to the cosmological origin of GRB and their enormous energy outputs. In most cases the red shifts have been measured in the faint host galaxies. The list of red shift measurements is given in the Table 1, where data about redshifts from Djorgovski et al. (2001) are completed by total GRB fluences (Bisnovatyi-Kogan 2003). This table contains the trigger number and fluence from 4B catalogue (Paciesas et al. 1999), and fluence for the GRB from other references. Huge energy output during a short time (0.1 – few 100 seconds) create problems for the cosmological interpretation.

It was shown first by Paczynski (1998), that properties of GRB afterglows are explained better under suggestion that GRB source is situated in a dusty star forming region with a high gas density. Interaction of mighty GRB pulse with the surrounding gas with a density $n = 10^4 - 10^5 \text{ cm}^{-3}$ create a specific form of the optical afterglow, lasting up to few tens of years. The calculations of light curve and spectrum of such afterglow have been done by Bisnovatyi-Kogan & Timokhin (1997). Some results are represented in Fig. 3. It was shown, that counterparts of cosmological GRB due to interaction of gamma-radiation with dense interstellar media are “long-living” objects, existing for years after GRB. To distinguish GRB counterpart from a supernova event, having similar energy output, it is necessary to take into account its unusual light curve and spectrum. In the optical region of the spectrum the strongest emission lines are H_α and H_β . Discovery of even one optical counterpart of GRB with properties described above would give an opportunity to probe the density of the interstellar medium around the burst, and therefore would give an indication of the burst progenitor.

3.3 Collimation

To avoid a huge energy production strong collimation is suggested in the radiation of GRB. In the “cannon-ball” model of Dado et al. (2002) the bulk motion Lorentz factor is $\Gamma \approx 10^2 - 10^3$, leading to collimation factor $\Omega \approx 10^{-4} - 10^{-6}$. Analysis of GRB collimation have been done by Rhoads (2001). The main restriction to the collimation angle follows from the analysis of the probability of appearance of the orphan optical afterglow, which most probably have low or no collimation. The absence of any variable orphan afterglow in a search poses the following restrictions. It was expected to detect ~ 0.2 afterglows, if bursts are isotropic, so the absence of orphan afterglows suggests $\Omega_{\text{opt}}/\Omega_\gamma \ll 100$, which is enough to rule out the most extreme collimation scenarios. At radio wavelengths published source counts and variability studies have been used by Perna and Loeb (1998) to place a limit on the collimation angle, $\theta_\gamma \geq 5^\circ$. Because radio afterglows last into the non-relativistic phase of the GRB remnant evolution, the radio afterglows are expected to radiate essentially isotropically, and the orphan afterglow limits on radio Ω_r/Ω_γ immediately imply a limit on Ω_γ itself.

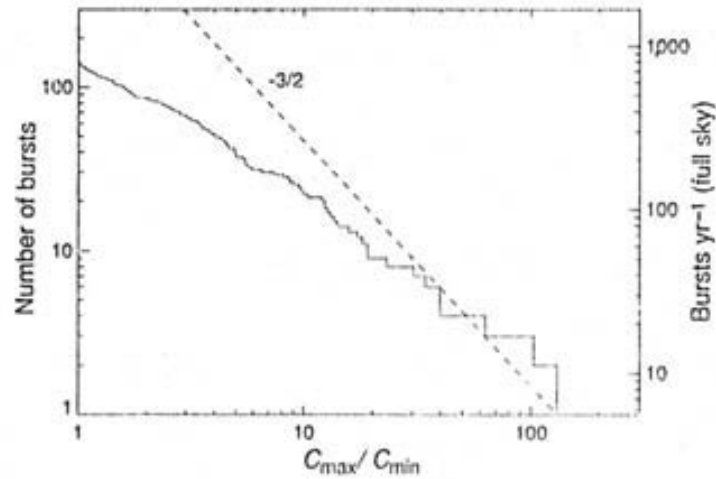


Fig. 1 Integral number distribution of 140 GRB as a function of peak rate. A $-3/2$ power law is expected for a homogeneous distribution of sources. The full sky rate is ~ 800 bursts per year, from Meegan et al. (1992).

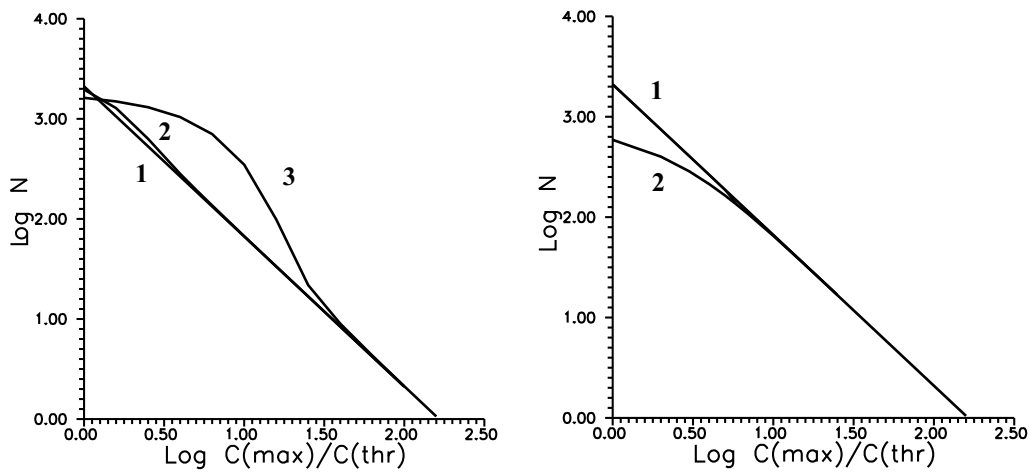


Fig. 2 a. The curve $[\log N - \log C(\max)/C(\text{thr})]$ in presence of stochastic errors, distributed according to normal distribution with an average error Δ_1 in units of a threshold; 1 – straight line with slope $3/2$, corresponding to $\Delta_1 = 0$; 2 – curve with $\Delta_1 = 1$; 3 – curve with $\Delta_1 = 10$. **b.** Same as in **a** for normal logarithmic distribution, Δ determines a logarithm of number of thresholds, as an average error; 1 – straight line with a slope $3/2$, corresponding to $\Delta = 0$; 2 – curve with $\Delta = 1$; $C(\max)$ is the peak intensity of the burst; $C(\text{thr})$ is a corresponding threshold value, from Bisnovaty-Kogan (1997).

Table 1 GRB Host Galaxies, Redshifts and Fluences (June 2001)

Trigger number	GRB	R mag	Redshift	Type ^a	Fluence ^e erg cm ⁻²
	970228	25.2	0.695	e	10 ⁻⁵
6225	970508	25.7	0.835	a, e	3.5 × 10 ⁻⁶ (3+4)
6350	970828	24.5	0.9579	e	7 × 10 ⁻⁵
6533	971214	25.6	3.418	e	10 ⁻⁵ (3+4)
6659	980326	29.2	~1?		6.3 × 10 ⁻⁷ (3+4)
6665	980329	27.7	<3.9	(b)	7.1 × 10 ⁻⁵ (3+4)
6707	980425 ^c	14	0.0085	a, e	4.4 × 10 ⁻⁶
6764	980519	26.2			9.4 × 10 ⁻⁶ (all 4)
	980613	24.0	1.097	e	1.7 × 10 ⁻⁶
6891	980703	22.6	0.966	a, e	5.4 × 10 ⁻⁵ (3+4)
7281	981226	24.8			2.3 × 10 ⁻⁶ (3+4)
7343	990123	23.9	1.600	a, e	5.1 × 10 ⁻⁴
7457	990308 ^d	>28.5			1.9 × 10 ⁻⁵ (3 + 4)
7549	990506	24.8	1.30	e	2.2 × 10 ⁻⁴
7560	990510	28.5	1.619	a	2.6 × 10 ⁻⁵
	990705	22.8	0.86	x	~ 3 × 10 ⁻⁵
	990712	21.8	0.4331	a,e	
	991208	24.4	0.7055	e	~ 10 ⁻⁴
7906	991216	24.85	1.02	a, x	2.1 × 10 ⁻⁴ (3+4)
7975	000131	>25.7	4.50	b	~ 10 ⁻⁵
	000214		0.37–0.47	x	~ 2 × 10 ⁻⁵
	000301C	28.0	2.0335	a	~ 4 × 10 ⁻⁶
	000418	23.9	1.1185	e	1.3 × 10 ⁻⁵
	000630	26.7			2 × 10 ⁻⁶
	000911	25.0	1.0585	e	5 × 10 ⁻⁶
	000926	23.9	2.0369	a	2.2 × 10 ⁻⁵
	010222	>24	1.477	a	brightest of BeppoSAX

Notes:

^a e = line emission, a = absorption, b = continuum break, x = x-ray^c Association of this galaxy/SN/GRB is somewhat controversial^d Association of the OT with this GRB may be uncertain^e The number of BATSE peak channel is indicated in brackets, from 1999, otherwise the estimation of bolometric fluence from other sources, made in 2003 is indicated

Comparison of the red shifts and fluences from Table 1 shows no correlation between distance and observed flux (see Fig. 4). It is explained by strong collimation, and strong scattering is connected with different sight angles in the beam. If the collimation is connected with the relativistic bulk motion (Dado et al. 2002), than strong correlation is expected between GRB duration and their power: stronger GRB should be shorter. Absence of such correlation excludes models based on the relativistic bulk motion collimation.

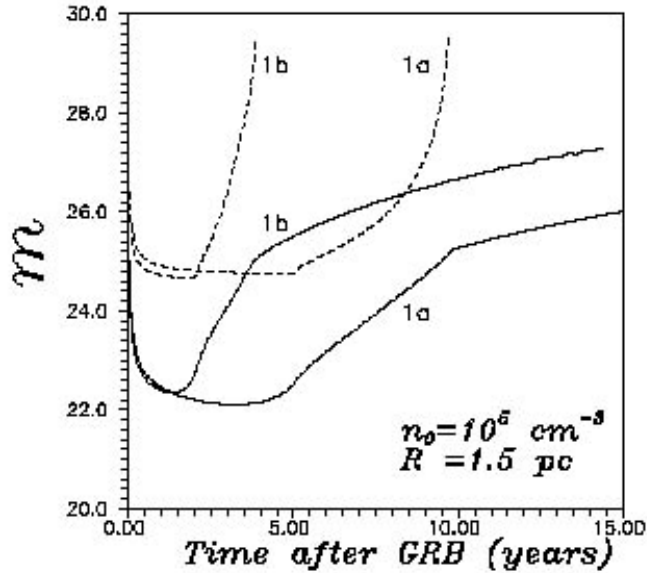


Fig. 3 The magnitudes of the counterparts (upper limit – solid line, lower limit – dashed line) as a function of time after burst for GRB with total flux near the Earth $F_{\text{GRB}} = 10^{-4} \text{ erg cm}^{-2}$: 1a. – for the case $E = 10^{52} \text{ erg}$; $n_0 = 10^5 \text{ cm}^{-3}$; 1b – for the case $E = 10^{51} \text{ erg}$; $n_0 = 10^5 \text{ cm}^{-3}$, from Bisnovaty-Kogan and Timokhin (1997).

3.4 Prompt Optical Afterglows

The afterglow of GRB 990123 was caught by optical observations 22 seconds after the onset of the burst (Akerlof et al. 1999, 1999). GRB 990123 was detected by BATSE on 1999 January 23.407594. The event was strong and consisted of a multi-peaked temporal structure lasting $\geq 100 \text{ s}$ (see Fig. 5), with significant spectral evolution. The T50 and T90 durations are $29.82 (\pm 0.10) \text{ s}$ and $63.30 (\pm 0.26) \text{ s}$, respectively. The maximum optical brightness 8.95^m was reached 30 s. after the GRB beginning, and after 95 s. it was already of 14.5^m . So the gamma ray maximum almost coincides with the optical one. The observed optical luminosity, related to the red shift $z = 1.61$ reaches $L_{\text{opt}} \approx 4 \times 10^{49} \text{ erg s}^{-1}$, what is about 5 orders of magnitude brighter than optical luminosity of any observed supernova. The energy of the prompt optical emission reaches 10^{51} erg , and the isotropic gamma-ray flux is about $2.3 \times 10^{54} \text{ erg}$, what exceeds the rest energy of the Sun (Akerlof et al. 1999; Kulkarni et al. 1999). Another bright afterglows have been observed in GRB 021004 (15 m, $z = 2.3$), GRB 030329 (12.4 m, $z = 0.168$) and GRB 030418 (16.9 m). Brightest visual magnitude and redshift are given in brackets. The most remarkable afterglow observed by many observatories was in GRB 030329 (see i.g. Rumjantsev et al. 2003; Burenin et al. 2003), where supernova was probably detected by the features of spectra (Stanek et al. 2003). Konus-Wind observations of GRB 030329 are given in Fig. 6, and light curve of the optical afterglow obtained in Crimea observatory is represented in Fig. 7 (from Pozanenko 2003).

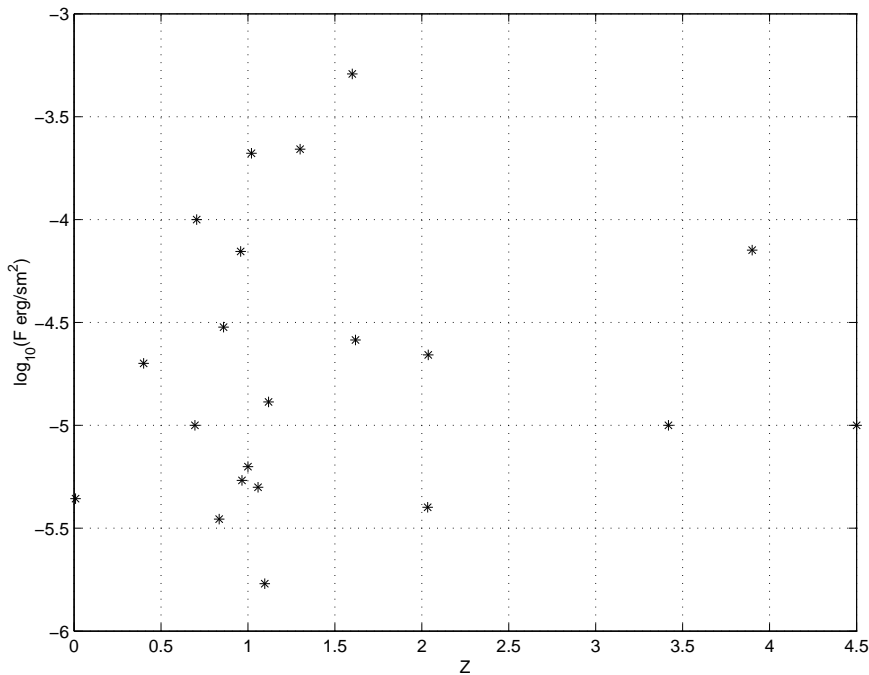


Fig. 4 Fluence F versus redshift z for GRB from the Table 1.

3.5 High-Energy Afterglow

EGRET observations on CGRO have shown that GRB emit also very hard gamma photons up to 20 GeV (Fishman & Meegan 1995). The number of GRB with detected hard gamma radiation is about 10, from them 5 bursts had registered photon energies over 100 MeV (Schneid et al. 1995). Hard gamma emission continues up to 1.5 hours in the GRB940217. Comparison of the angular aperture of EGRET and BATSE leads to conclusion that hard gamma radiation could be observed in large fraction (about one half) of all GRB. Spectral slope in hard gamma region lays between (-2) and (-3.7) , and varies rapidly, becoming softer with time (GRB 920622 in Schneid et al. (1995)). Data about spectra of hard gamma radiation of radio pulsars in Crab nebula (Much et al. 1996), and PSRB1055-52 (Thompson et al. 1999) show similar numbers and variety. With account of non-pulsed Crab spectrum the slope varies between (-1.78) and (-2.75) . If GRB is connected with SN explosion and neutron star formation, than residual oscillations of the neutron star may be responsible for the extended hard gamma ray afterglow (Bisnovatyi-Kogan 1995; Timokhin et al. 2000, Ding & Cheng 1997).

3.6 Hard X-Ray Lines

Hard gamma-ray lines in GRB spectra have been discovered by KONUS group (Mazets et al. 1982a). They had been interpreted there as cyclotron lines, and have been seen in 20% – 30% of the GRB. These spectra had shown a distinct variability: the visible absorption decreases with time (Fig. 8). In BATSE data existence of hard X-ray spectral features in GRB spectra was

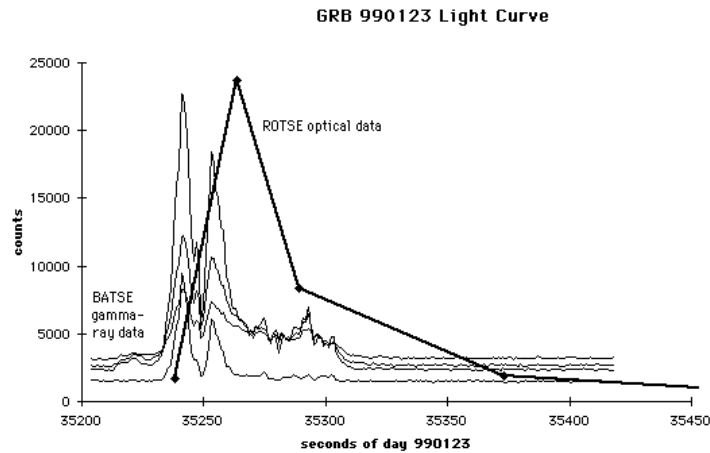


Fig. 5 Thin lines represent BATSE gamma-ray profile with 1024 ms resolution in different energy channels. The thick line represents the first few frames of ROTSE data. ROTSE began taking data 22 seconds after the initial trigger. This is the brightest ever optical burst, from Pozanenko, (2003).

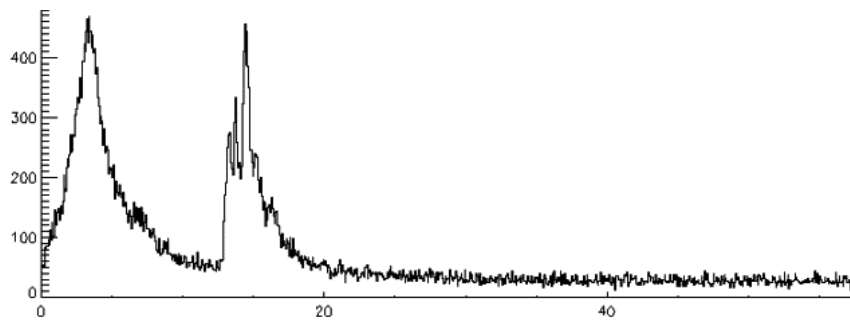


Fig. 6 GRB030329 in gamma-ray: Konus-Wind 11:37:29 UT. Fluence = 1.2×10^{-4} erg cm^{-2} , Duration=50 s, Peak Flux = 2.5×10^{-5} erg cm^{-2} s^{-1} ; One of the most luminous burst (from 4000). From Pozanenko (2003).

found by Briggs et al. (1999). In this paper 13 statistically significant line candidates have been found from 117 investigated GRBs. One of the best cases for detecting a line is GRB 941017 in which the data from two detectors are consistent. In some GRBs the line was found only by one detector, while it was not statistically significant in the other one. The data for GRB 930916 from the detector with the well observed line is given in Fig. 9 from Briggs et al. (1999). The conclusion of this paper is that the reality of all of the BATSE line candidates is unclear. Note however that spectra of GRB 930916 had been obtained 20 s after the trigger, and according to Mazets et al. (1982a) the lines are the strongest at the beginning of the burst (see Fig. 8). The

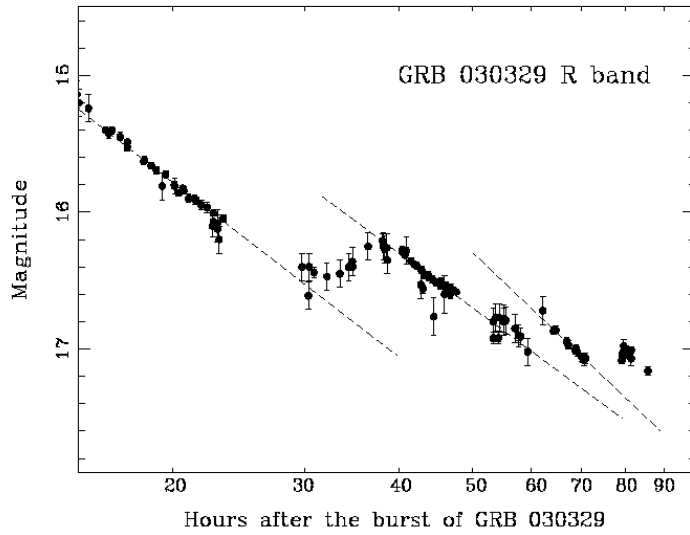


Fig. 7 Variability in hours scale of the optical afterglow of GRB030329, from Pozanenko, (2003).

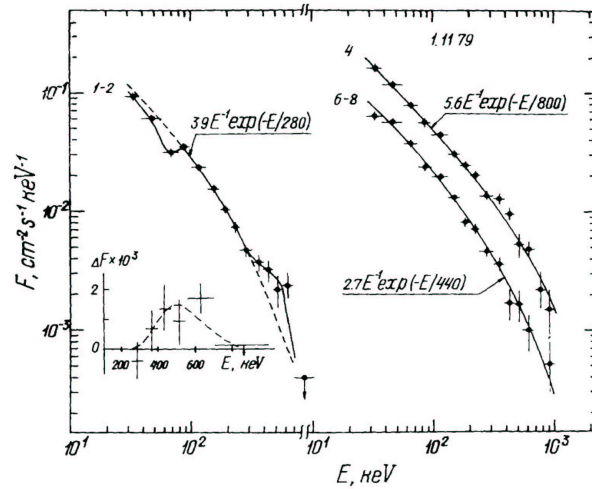


Fig. 8 Spectral evolution of 1 November 1979 burst. (1–2) spectrum obtained in the first 8 s with absorption line at ≈ 65 keV and broad emission feature at 350–650 keV; (4) spectrum measured in the 4-th 4 s interval; (6–8) spectrum summed over 6-th, 7-th and 8-th intervals, from Mazets et al. (1982b).

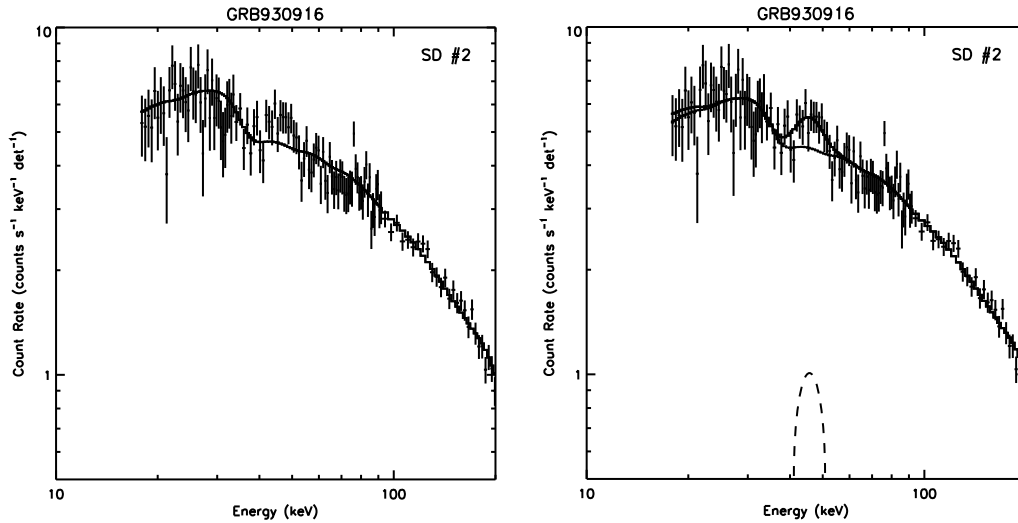


Fig. 9 Data from the interval 22.144 to 83.200 s after the BATSE trigger of GRB930916. The ‘bump’ at 30 keV is expected from the K-edge of the iodine in NaI. Left panel: best continuum-only fit to the data of SD 2. Right panel: A narrow spectral feature is added to the model: an emission line at 45 keV improves χ^2 by 23.1. The solid histogram depicts the total count model; the dashed histograms show the continuum and line portions separately, from Briggs et al. (1999).

only interpretation in the cosmological model (Hailey et al. 1999) is based on the blue-shifted ($\Gamma = 25 - 100$) spectrum of the gas cloud illuminated by the gamma radiation of the fireball. Similar model was suggested by Bisnovaty-Kogan & Illarionov (1989) for explanation of the lines observed by KONUS.

3.7 GRB and Supernovae

The following GRB have evidences for their connection with SN: GRB 980425 ($z = 0.0085$, 40 Mpc), GRB 980326 ($z = 1$), GRB 011121 ($z = 0.365$), GRB 020405 ($z = 0.695$), GRB 030329 ($z = 0.169$). Some optical afterglows have a red bump? during 15–75 days, what may be consistent with the underlying SN explosion, see i.g. Sokolov (2001). Nevertheless the SN-GRB connection is not quite certain.

4 SHORT GRB AND SGR

The statistical analysis reveals at least two separate samples consisting of long ($> \sim 2$ s) and short bursts. Optical afterglows and redshift measurements have been done only for long bursts. Therefore, it is not excluded that short bursts have different (may be galactic) origin. Compare properties of short GRB with giant bursts from soft gamma-repeaters (SGR) inside the Galaxy. From the larger distance only giant bursts would be registered, which could be attributed to short GRB. The existence of giant bursts in the SGR (3 in 4 firmly known SGR in the Galaxy and LMC) implies a possibility for observation of giant bursts, which appear as short GRB, in

other neighboring galaxies. The estimation gives more than 10 expected “short GRB” of this type from M31 and other close neighbors. The absence of any GRB projecting on the local group galaxies may indicate that SGR are more close and less luminous objects, than it is now accepted (Bisnovatyi-Kogan 2002).

5 CONCLUSIONS

There is no fully consistent GRB model: neither radiation, nor explosion. It is not excluded, that short GRB have galactic origin, and giant bursts in SGR are connected with short GRB (Mazets et al. 1982b). Critical experiments are needed: spectra of prompt optical afterglows; study of hard gamma-ray afterglows; search for orphans optical afterglows in optical all sky monitoring. Cosmological GRB may come from collapse of massive rotating star followed by formation of Kerr black hole surrounded by massive magnetized disk, and rapid accretion leading to GRB; or from some exotic models.

Acknowledgements The author is grateful to F. Giovannelli and the organizers of the workshop for support and hospitality. Author acknowledges partial support from RFBR grant 02-02-16900 and INTAS grant 00491.

References

- Akerlof C. W. et al., 1999, *Nature*, 398, 400
 Akerlof C. W., McKay T. A., 1999, *GCN205*
 Ardeljan N. V., Bisnovatyi-Kogan G. S., Moiseenko S. G., 1997, *Physics-Uspekhi*, 40, 1076
 Ardeljan N. V., Bisnovatyi-Kogan G. S., Moiseenko S. G., 2000, *A&A*, 355, 1181
 Berezinsky V. S., Prilutsky O. F., 1987, *A&A*, 175, 309
 Bisnovatyi-Kogan G. S., 1971, *Sov. Astron.*, 14, 652
 Bisnovatyi-Kogan G. S., 1995, *ApJS*, 97, 185
 Bisnovatyi-Kogan G. S., 1997, *A&A*, 324, 573
 Bisnovatyi-Kogan G. S., 2002, *Proc Vulcano99 Workshop: Mem. Soc. Astron. It.*, 73, 318
 Bisnovatyi-Kogan G. S., 2003, *Proc Vulcano2002 Workshop* (in press); *astro-ph/0310361*
 Bisnovatyi-Kogan G. S. and Illarionov A. F., 1989 *A&A*, 213, 107
 Bisnovatyi-Kogan G. S., Imshennik V. S., Nadyozhin D. K., Chechetkin V. M., 1975, *Ap&SS*, 35, 23
 Bisnovatyi-Kogan G. S. and Timokhin A. N., 1997, *Sov. Astron.*, 41, 423
 Briggs M. S. et al., 1999, *astro-ph/9901224*
 Burenin R. et al., 2003, *CGN2001*
 Dado S., Dar A., De Ru'jula A., 2002, *A&A*, 388, 1079
 Ding K. Y., Cheng K. S., 1997, *MNRAS*, 287, 671
 Djorgovski S. G. et al., 2001, *astro-ph/0107535*
 Fishman G. J., Meegan C. A., 1995, *Ann. Rev. Astron. Ap.*, 33, 415
 Hailey C. J., Harrison F. A., Mori K., 1999, *ApJLett.*, 520, L25
 Harrison T. E., Webber W. R., McNamara B. J., 1995, *Astron. J.*, 110, 2216
 Higdon J. C., Schmidt M., 1990, *ApJ*, 355, 13
 Kulkarni S. et al., 1999, *Nature*, 398, 389
 MacFadyen A. I., Woosley S. E., 1999, *ApJ*, 524, 262
 Mazets E. P. et al., 1980, *Sov. Astron. Lett.*, 6, 318
 Mazets E. P. et al., 1982a, *Ap&SS*, 82, 261

- Mazets, E. P., Golenetskii, S. V., Gurian, Iu. A., Ilinskii, V. N., 1982b, *Ap&SS*, 84, 173
- Meegan C. et al., 1992, *Nature* 355, 143
- Much R. et al., 1996, *A&AS*, 120, 703
- Paciesas W. S. et al., 1999, The Fourth BATSE Gamma-Ray Burst Catalog (Revised). On-line Data Catalog: IX/20A. Originally published in *ApJ Suppl.* 122, 465, 497
- Paczynski B., 1998, *ApJLett.*, 494, L45
- Perna R., Loeb A., 1998, *ApJLett.*, 509, L85
- Pozanenko A. S., 2003, Private communication
- Prilutsky O. F., Usov V. V., 1975, *Ap&SS*, 34, 387
- Rhoads J. E., 2001, *astro-ph/0103028*
- Ruffert M., Janka H.-Th., 1998, *A&A*, 338, 535
- Ruffert M., Janka H.-Th., 1999, *A&A*, 344, 573
- Ruffini R. et al., 2000, *A&A*, 359, 855
- Rumjantsev V. et al., 2003, GCN2005
- Schmidt M., 1999, *ApJLett.*, 523, L117
- Schmidt M., 2001, *ApJ*, 552, 36
- Schneid E. J. et al., 1995, *Ann. NY Acad. Sci.*, 759, 421
- Schneid E. J. et al., 1995, *ApJ*, 453, 95
- Sokolov V. V., 2001, *astro-ph/0102492*
- Stanek K. Z. et al., 2003, *ApJLett.*, 597, L17
- Thompson D. J. et al., 1999, *ApJ*, 516, 297
- Timokhin A. N., Bisnovaty-Kogan G. S., Spruit H. C., 2000, *MNRAS*, 316, 734
- Usov V. V., 1992, *Nature* 357, 472
- van Putten M. H. P. M., 2001 *Phys. Rep.* 345, 1